REMOTE SENSING AS A PRELIMINARY ANALYSIS FOR THE DETECTION OF ACTIVE TECTONIC STRUCTURES: AN APPLICATION TO THE ALBANIAN OROGENIC SYSTEM

DALJINSKA ISTRAŽIVANJA KAO PRELIMINARNA METODA ZA OTKRIVANJE AKTIVNIH TEKTONSKIH STRUKTURA: PRIMJER ALBANSKOG OROGENA

ANDREA FAVRETTO[1], RICCARDO GELETTI[2], DARIO CIVILE[2]

[1] *GIS Laboratory – University of Trieste*
[2] *The National Institute of Oceanography and Experimental Geophysics (OGS) - Trieste*

UDK: 551.4:528.8(496.5)=111
Primljeno / *Received*: 2013-08-26
Izvorni znanstveni rad
Original scientific paper

As is well known, both the traditional direct geological and geophysical survey methods used to identify geologic features are very expensive and time-consuming procedures.

In this regard, remote sensing methods applied to multispectral and medium spatial resolution satellite images allow a more focused approach with respect to the more specific geologic methods. This is achieved by a preliminary land inspection carried out by the semi-automated analysis of satellite imagery. This avoids wasting resources as the geological/geophysical survey methods can be later applied only to those zones suspected of having certain tectonic activity (derived by the remotely sensed imagery).

This paper will evaluate an ASTER sensor satellite image (and its derived Digital Elevation Model or DEM), in order to point out the suspected presence of active geologic structures (faults). The area in question is west – central Albania. The results of the remote sensing procedures are later compared with the established data for the same area taken by satellite images, in order to verify the reliability of the adopted method. The source of the established data has been from the bibliography.

Keywords: active faults, remote sensing, ASTER, Albania

Tradicionalne izravne geološke i geofizičke metode istraživanja koje se koriste za prepoznavanje geoloških obilježja su vrlo skupe i dugotrajne. U tom smislu metode daljinskh istraživanja za analizu multispektralnih satelitskih snimaka i snimaka srednje rezolucije omogućuju kvalitetniji pristup s obzirom na specifične geološke metode. U skladu s tim moguće je napraviti preliminarnu analizu površine tla putem poluautomatske analize satelitskih snimaka. Ovakva analiza omogućuje snižavanje troškova na način da se geološke/geofizičke metode istraživanja koriste naknadno, i to u onim područjima za koje se ovakvom analizom (korištenjem daljinskih snimaka) utvrdi postojanje određene tektonske aktivnosti.

U ovom radu analizira se satelitska snimka ASTER (i na temelju nje napravljen digitalni model reljefa – DMR) kako bi se uputilo na eventualnu prisutnost aktivnih geoloških struktura (rasjeda). Ovim istraživanjem obuhvaćeno je područje zapadne i središnje Albanije. Radi utvrđivanja pouzdanosti navedene metode rezultati analize snimaka dobivenih daljinskim istraživanjem su uspoređeni s postojećim podacima za isto područje dobivenima satelitskim snimanjem. Postojeći, istraživanjima potvrđeni podaci preuzeti su iz objavljene literature.

Ključne riječi: aktivni rasjedi, daljinska istraživanja, ASTER, Albanija

Introduction

As is well known, identifying the active faults in a certain area is fundamental before constructing important economic and network structures (pipelines, dams, roads, etc). This is mainly because the faults are seismogenic. Nevertheless, these surveys can be time-consuming and expensive, when carried out in a traditional way (geologic and/or *in situ* geophysical surveys). In this regard, we think that applying remote sensing technologies can constitute an ideal completion of traditional geological procedures (Sabins, 1996; Jensen, 2000; Gupta 2003). Our idea was to do some preparatory analysis on remotely sensed images, with the aim of selecting some areas with suspected geologic activity (active faults). The same areas, which have been discovered with these non-invasive and relatively cheap methods, will later be investigated with specific geological methods (geological and/or geophysical surveys). There are not many papers related to remote sensing applications with reference to these geological arguments, which use medium spatial resolution remotely sensed images and DEM (for instance: Fu et al. 2004; Walker, 2006; Perez et al., 2006; Tarolli et al., 2009).

This paper aims at contributing to the matter, through a concrete example located in a little-studied area using traditional geological methods. Our intention has been to focus on the method because of the fact that we analyzed a partially known area from the perspective of geological activity. Our geological bibliography knowledge formed both the starting point of the remote sensing procedures and the first verification of our results based on the image analysis.

We proceeded in the following way:

1. drew a vector layer of the principal fault lines of the studied area. The faults were derived from the geological/structural maps (scale 1:200.000) of the local geologic service and from the maps of the published papers we referred to;
2. drew a further series of vector layers, which indicate the location of two important geological sections (interpreted from seismic profiles). In addition to the geological size and orientation, they also register the principal underground rifts of the geological sections;
3. on the basis of the surface features of active thrusts and back thrusts that can be indicated by the elaboration of satellite imagery, we identified the suspected fault lines in the area;
4. the suspected fault lines detected via this method have been compared with the ones obtained by geophysical/geological methods (from the published papers and from the local geologic service). An additional check of the obtained results was also carried out through the geological section layer (mentioned at point 2 of this list).

The studied area is located in central-west Albania, between the Adriatic coast and the mountainous inland. This area has been chosen for its geological features. In fact, it is an area with a strong recent orogenic activity, which is ongoing (see part 2). We used two ASTER sensor (Terra satellite) images. Besides the two multispectral, medium spatial resolution images, we also used a DEM of the same area.

Geological setting

The development of the present day Albanian relief which, characterized by mountain belts up to over 2,000 m in height, is mainly the result of the Cenozoic contractional phases that led to the construction of the fold and thrust belt, known as Albanides. Moreover, the Pliocene to recent neotectonic activity of Albanides is accompanied by a strong and progressive uplift (Aliaj, 1998; Roure et al., 2004).

The Albanides are derived by the deformation of the eastern passive margin of Adria or Apulia microplate (Dewey et al., 1973; Makris, 1981; Stampfli, Mosar, 1999; Dercourt et al., 2000), constituted by carbonate platforms and deep-sea basins. In addition, the region contains an ophiolitic suture following the collision of the African and Eurasian plates (Vilasi et al., 2009; Jardin et al., 2011).

The Albanides are characterized by W-verging N–S to NW-trending thrusts and back thrusts and related folds (Roure et al., 2004). This area can be subdivided into two major structural domains: an eastern internal zone (Internal Albanides) and a western external zone (External Albanides) (Meço, Aliaj, 2000; Robertson, Shallo, 2000; Roure et al., 2004; Frasheri et al., 2009; Lacombe et al., 2009; Jardin et al., 2011). The Internal Albanides consist of Triassic and Jurassic thick-skinned thrust sheets, characterized by the presence of ophiolites (Mirdita Zone), deformed

by several Jurassic-Cenozoic tectonic phases. The External Albanides comprise the Krasta–Cukali, the Kruja, the Periadritaic Depression and the Ionian tectonic zones. The sedimentary succession of the Ionian Zone is affected by Oligo-Neogene tectonic phases. This geological formation mainly consists of Triassic evaporites, Jurassic-Cenozoic carbonates, Oligo-Pliocene flysch and post-orogenic siliciclastic deposits.

The study area includes the Ionian and the Sazani tectonic zones. The Ionian zone is characterized by steep and high mountains mainly consisting of Meso-Cenozic evaporates and carbonate rocks. The Sazani tectonic Zone (including the Karaburun Peninsula and Sazan Island) represents the outcropping portion of the carbonate foreland (Apulian carbonate platform), affected by contractional deformation and involved in the chain (Velaj et al., 1999; Meço, Aliaj, 2000; Nikolla et al., 2002; Roure et al., 2004). This zone is morphologically characterized by a NE-trending ridge which is up to 1,400 m high, including also the Sazan Island, with very pronounced coastal cliff. The investigated sector is bounded to the north by the main NE-trending transversal fault zone, named Vlora Elbasani-Dibra. The Vlora-Elbasan-Dibra transfer zone (Roure et al., 2004, Vilasi et al., 2009) separates two distinct tectonic provinces in the Extrernal Albanides: the Peri-adriatiac Depression in the north, from the deformed Mesozoic carbonates of the Ionian Zone in the south (Bakia, Bega, 1989; Velaj et al., 1999; Robertson, Shallo, 2000; Nieuwland et al., 2001; Roure et al., 2004; Lacombe et al., 2009). Another important transversal fault zone is the Shkoder-Peja in the north of Albania (Zelilidis et al., 2003; Roure et al., 2004) which marks the boundary between the Dinarides and Albanides-Hellenide domain.

Albania is one of the most seismically active countries in Europe. In fact, the intense present-day seismic activity recorded both in onshore and offshore (Aliaj et al., 2000, 2004; Nieuwland et al., 2001; Sulstarova, Aliaj, 2001; Kiratzi, Muço, 2004; Vannucci et al., 2004) and the GPS data (Hollenstein et al., 2003; Jouanne et al., 2012) indicate that the Albanides are currently deforming. This tectonic activity controlled the recent evolution of the landscape generating morphological features, as in the case of the study area, that can be identified by satellite methods.

Methods

Cartographic Database

We used the following satellite images:

- two ASTER sensor satellite images, taken on 23/09/2003 and 11/04/2007 (AST_L1B product); each image is about 60 square km wide and is georeferenced in the WGS84/UTM 34N coordinate system. As is well known, the ASTER sensor takes images of the Earth in 14 different wavelengths of the electromagnetic spectrum, ranging from visible to thermal infrared light. The spatial resolution ranges from 15 meters with the VNIR system (first three bands: green, red, near infrared) to 30 meters with the SWIR system (medium infrared), to 90 meters with the TIR system (thermal infrared);[1]
- Digital Elevation Model – DEM (ASTER Global Digital Elevation Model – GDEM product), elaborated from ASTER images by NASA together with SILC (Japan's Sensor Information Laboratory Corporation.[2] The DEM layer was provided by LP DAAC (Land Processes Distributed Active Archive Center – https://lpdaac.usgs.gov/). It is georeferenced in lat/long coordinates (Datum WGS84). Its spatial resolution is 30 meters.

The following vector layers have been added to the raster images:

- one linear vector layer showing the location of some of the main fault lines in the area. The fault lines were derived by geophysical/geological methods and were taken from the official geological Albanian cartography (Xhomo et al., 1999; Xhomo et al., 2002). The fault lines have been updated with the ones taken from the maps of Aliaj et al. (2000), Carcaillet et al. (2009), Velaj (2011). The result was the summary of the "state of the art" of the underground active structures in the chosen area[3];

[1] See https://lpdaac.usgs.gov/products/aster_products_table/ast_l1b.

[2] See https://lpdaac.usgs.gov/products/aster_products_table/astgtm).

[3] The tectonic map of Albania has been scanned and georeferenced in the WGS84/UTM34N coordinate system. Using the WGS84/UTM34N coordinate system map, we obtained a vector layer with the principal fault lines of the area. The fault lines taken from the maps of Aliaj, Carcaillet and Velaj papers were later added to the same vector layer.

- one linear vector layer showing the location of two geological sections (interpreted from seismic profiles and taken from Aliaj, 2006 and Arapi 2012). We also placed the points indicating the existence of a fault along the geological sections.

Preliminary preparation of the satellite imagery

The 14 GeoTIF layers of each ASTER image have been stacked in a single image file. The SWIR and TIR system layers have been resampled to 15 meters VNIR pixel spatial resolution. Then we prepared a mosaic of the two ASTER scenes. In regards to the DEM, its layer has been transformed into the WGS84/UTM34N coordinate system.

Figure 1 shows the mosaic of the two ASTER images (Fig. 1B ZONE 1). The mosaic has been overlaid on the DEM layer (Fig. 1B ZONE 2), displayed in green and white colors (green: low ground elevation; white: high ground elevation). The same figure also features a map showing the location of the studied area in the Balkans (Fig. 1A), with reference to the principal geological/structural areas in the territory (Carcaillet et al., 2009).

Figure 2 shows all the prepared vector layers, which have been overlaid on the Albanian geological map. As it can be seen, along the linear geological sections we have added two geological section outlines (derived from seismic profiles - Aliaj, 2006; Arapi 2012). Finally, a photo point indicating the position of an active fault in the area has been added onto the geological map (Fig. 2 C – source: Dario Civile).

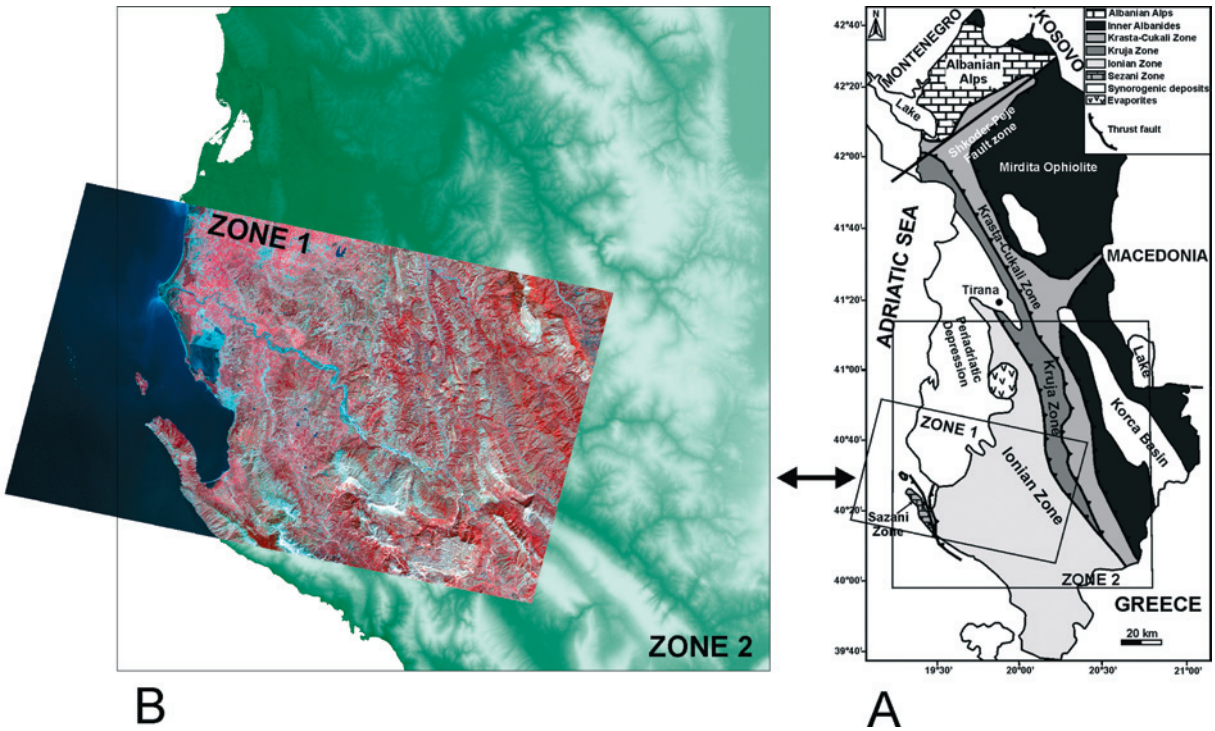

Figure 1 A) Structural sketch map of the Albania showing the main tectonic zones (modified from Lacombe et al., 2009) and the geographical location of the study area (inset). B) Satellite images where the ZONE 1 is the ASTER data showed in figs. 2, 3, 4, 7, 8 and the ZONE 2 is the DEM showed in figs. 5 & 6

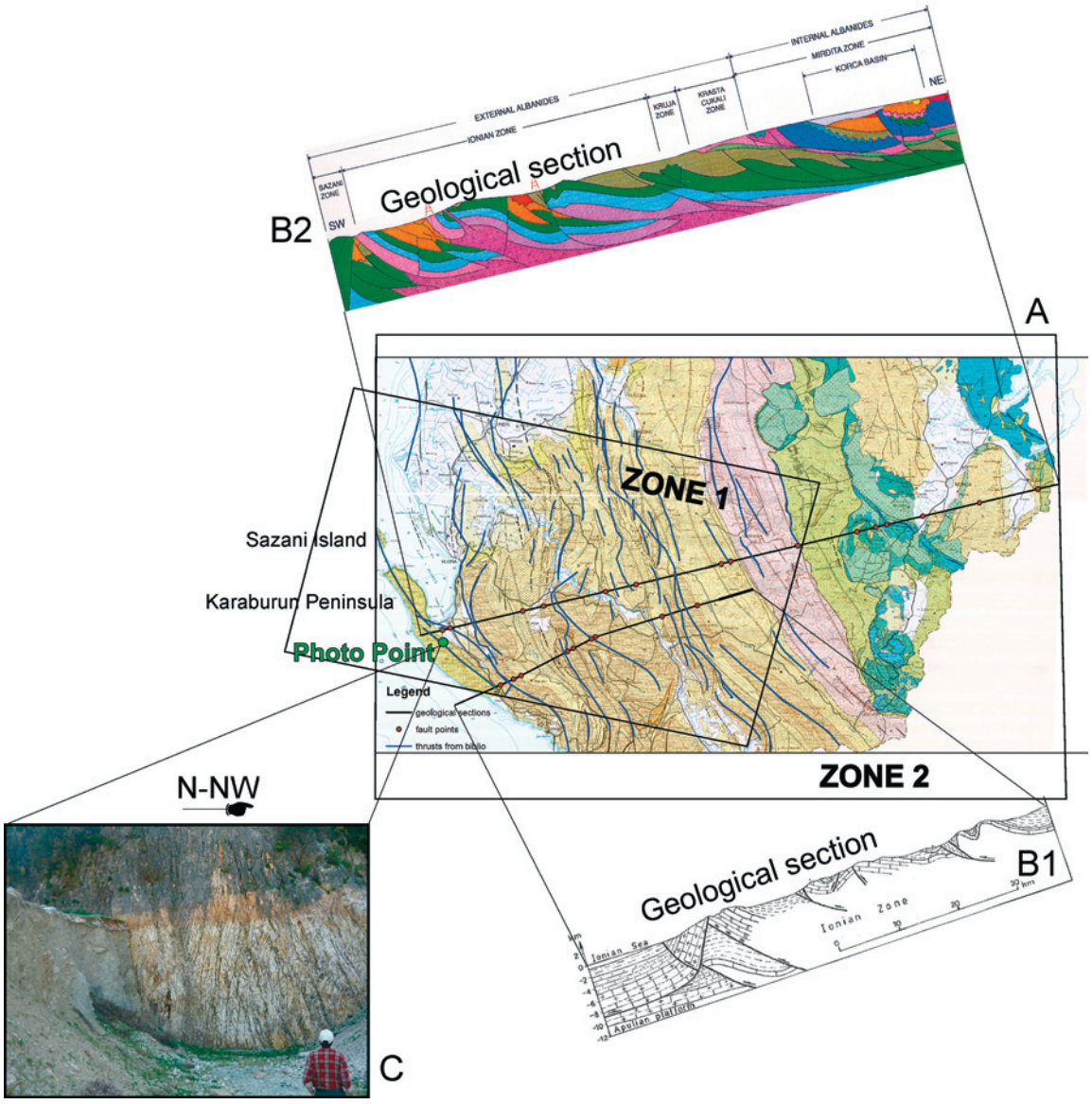

Figure 2 A) Geological map of the Central Albania (Geological map of Albania, scale 1:200,000, published by the Ministry of Industry and Energy, Republic of Albania, Xhomo et al., 2002) showing the main geological formations and faults. The B1) and B2) profiles on the map are an example of geological schematic cross-sections respectively modified after Arapi, 2012 and Aliaj, 2006, used for to verify the result of the interpretation of the satellite data; C) photo of an example of thrust fault surface located by this work

Methodology

Geological remote sensing has been used since the advent of artificial satellites (with active and passive sensors on board) in order to map territory (geological mapping), but also to recognize underground structures and so help the prospecting for hydrocarbons (for an almost thirty-year review of geology and remote sensing interfacing, see Van der Meer et al., 2011).

Of course, the analyses carried out on the satellite imagery are related to the aim of the paper, namely the identification of areas with suspected active faults inside. As noted, faults allow the transfer of underground water. The presence of underground water influences some surface parameters, which can be partly observed by remote sensing (see Papadaki et al., 2011). Among the surface features, which can show fault presence, we considered:

- soil moisture content, which can be outlined by sudden vegetation discontinuity or alignments;
- surface temperature;
- orographic alignments.

The different surface variables and the way they appear may indicate the presence of an underground fault. This high variability of surface structure and shapes suggests a visual check by a geology expert operator and reduces the application of automated remote sensing procedures. This can explain and justify the adopted methodology.

On the basis of the surface features recalled, we created some additional layers generated by the semi-automated procedures applied to the satellite imagery. These semi-automated procedures are, as follows:

- Vegetation Index. Vegetation index is a "dimensionless, radiometric measure that functions as an indicator of relative abundance and activity of green vegetation…" (Jensen, 2000). There are several vegetation indices in use. Among them, we chose the Normalized Difference Vegetation Index – NDVI, developed by Rouse et al. in 1974, which relates the near-infrared and visible reflectance of Earth surface features. NDVI has been widely adopted since its formulation and it "is preferred to the simple near infrared/red ratio ….because the ratio value is not affected by the absolute pixel values in the near-infrared and red bands" (Mather, 1999). Its values range from -1 to +1. High NDVI values "reveals pixels dominated by high proportion of green biomass" (Campbell, 1996). In contrast, negative index values are related to clouds, water and snow; index values near zero are related to rock and bare soil land cover (Lillesand, Kiefer, 1994).
- Principal Component Analysis – PCA. As it is well known, in a multispectral sensor such as ASTER, the digital numbers (DN) recorded by each band of the sensor are often correlated. This may imbue the different layers, which constitute the remotely sensed image, with a certain information redundancy (see Lillesand, Kiefer, 1994). PCA can eliminate the information redundancy and create a new set of layers, which are the principal components of the original bands, uncorrelated and with maximum variance. The new data set has a reduced dimensionality without the loss of information. Furthermore, PCA processed images may be more easily interpreted than the original spectral bands, displayed three by three with a conventional RGB system. This data compression property is useful if more than three spectral bands are available. In the case of an ASTER image, nine different spectral bands are available (plus five thermal bands), so it is very useful that the information of the whole dataset is compressed in three components (bands). The PCA images can be analyzed one by one or can generate an "RGB false-color composite in which principal component number 1 is shown in red, number 2 in green and number 3 in blue. Such an image contains more information than any combination of three spectral bands" (Mather, 1999). PCA has been diffusely applied to ASTER sensor images by geologists. Among others we can mention: Crosta et al., 2003; Gomez et al., 2005; Moore et al., 2008; Wahi et al., 2013).
- Terrain information on the basis of some DEM elaborations. It is well known that this kind of information depends strongly on the quality of topographic data (in this case the DEM). ASTER provides medium resolution (30 meters squared pixels) terrain data from photogrammetric processing of stereo VNIR bands (see, among others, Tarolli et al., 2009). The DEM layer has been elaborated in order to build two derived layers: slope and aspect.

We visually checked all the produced layers in order to isolate the suspected faults. Then the suspected faults have been drawn on the result vector layer. Finally, this vector layer has been compared with the starting vector layer, obtained through traditional geological analysis.

Results

Elaboration of the satellite imagery

NDVI – Normalized Difference Vegetation Index: using the red and near infrared ASTER bands (band 2 and band 3, respectively), NDVI has been calculated on the whole mosaic of the two ASTER images. In light of the fact that the following thrust research has been made in a visual way, we did not classify the NDVI layer. We only applied the linear stretching method to the whole NDVI value interval (-1 / +1) in order to gain a better display in the LUT (Look Up Table) between -0.4 /+0.4. Figure 3 shows NDVI applied to the

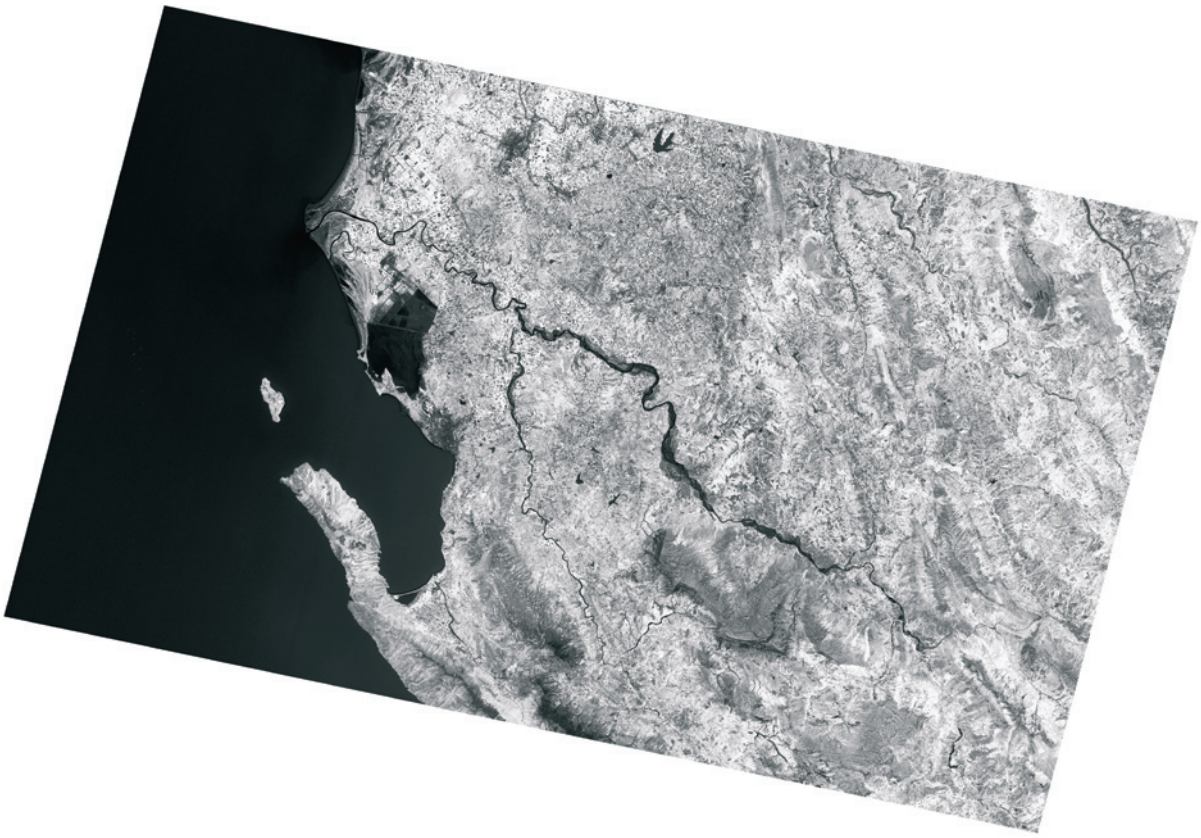

Figure 3 NDVI (Normalized Vegetation Difference Index) applied to the two ASTER image mosaic. NDVI values are displayed in gray tones (dark gray/black: absence of vegetation, light gray/white: bare soils to high vegetation)

mosaic of the ASTER images. NDVI values are displayed in gray tones (dark gray/black: absence of vegetation, light gray/white: bare soils to high vegetation).

PCA – Principal Component Analysis: in this study, as mentioned earlier, the visual analysis of the operator is very important and so may be the principal component analysis applied to the raw values of the sensor bands. In this particular case, we applied PCA to the first 9 bands of the sensor (the VNIR and SWIR systems). We did not consider the TIR system because their bands have been further analyzed in order to isolate the thermal factor. Besides, we decided to keep only the first three components of the VNIR/SWIR system for the further visual analysis, because they explained 99.18% of the total variance. Figure 4 shows the first three PCA displayed in gray tones (frames 1, 2, 3). Frame 4 shows the same three components displayed in RGB (red: PCA1, green: PCA2, blue: PCA3). As we stated before, this color combination can be considered the most informative one with respect to all possible combinations using the starting bands of the sensor. This is because each band (PCA1, 2, 3) is uncorrelated with the other two, and the three bands together explain almost the total variance of the scene. The information is nevertheless connected only to the geometry of the features, on the image, underlined by the color combination, and not to the image colors, useful in this case only for the contrast of the image. If we observe all the frames of Figure 4 (but especially frames 2, 3, 4), we can see two narrow columns where the pixels of the two mosaic ASTER images are irregular. This phenomenon occurs in the connection area of the two ASTER images and in the sides of the mosaic (especially the bottom right side). This can be explained by different spatial resolution of the two ASTER systems (VNIR and SWIR). As we know, VNIR has a spatial resolution of 15 meters, SWIR of 30 meters and TIR of 90 meters. This means that the different dimensions of the pixels of each ASTER band in the various systems (VNIR, SWIR and TIR), which are aligned

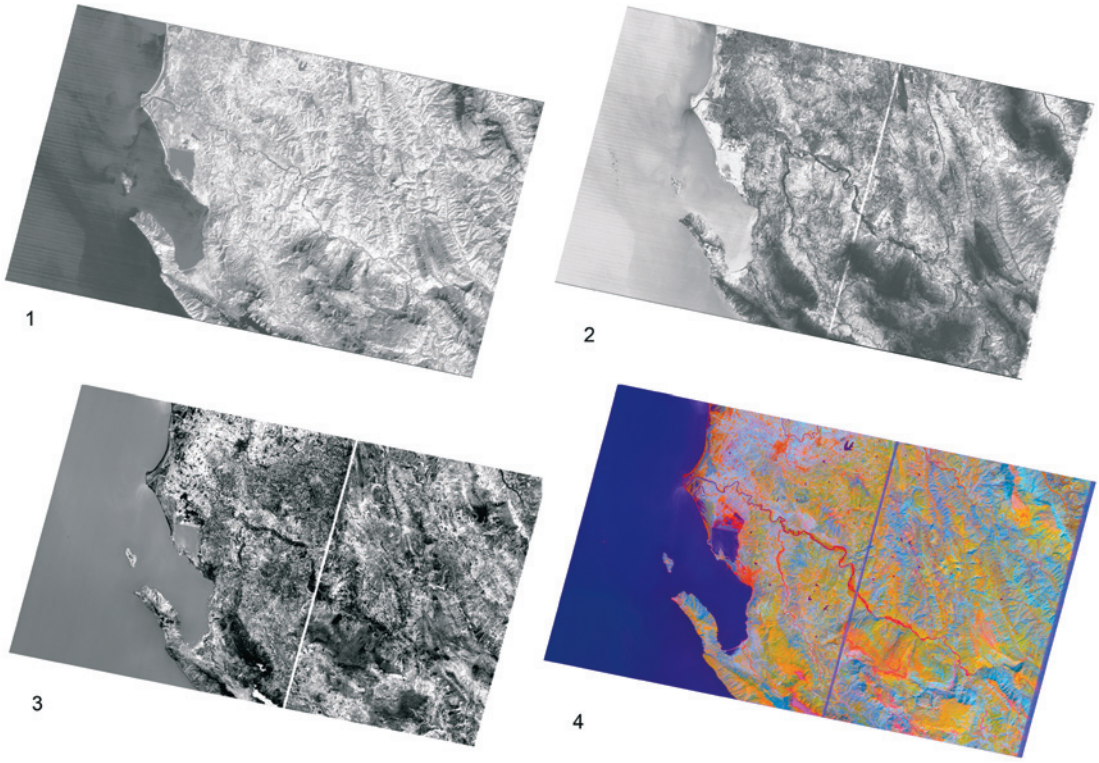

Figure 4 Frames 1, 2, 3) the first three principal component layers of the VNIR/SWIR ASTER bands displayed in gray tones (frame 1-PCA1, frame 2 – PCA2, frame 3 - PCA3); frame 4) the first three principal components displayed as red (PCA1), green (PCA2), Blue (PCA3)

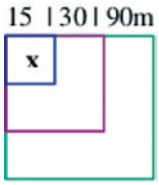

Figure 5 Diagram representing the upper-left pixel of each of the bands of VNIR, SWIR and TIR in an ASTER Level-1B data set

Source: USGS - NASA Land Processes Distributed Active Archive Center - LP DAAC, Geo-Referencing ASTER Level-1B Data: General Overview and Examples of Particular COTS Packages and Public Domain Software, (https://lpdaac.usgs.gov/sites/default/files/public/aster/docs/ASTER_GeoRef_FINAL.pdf)

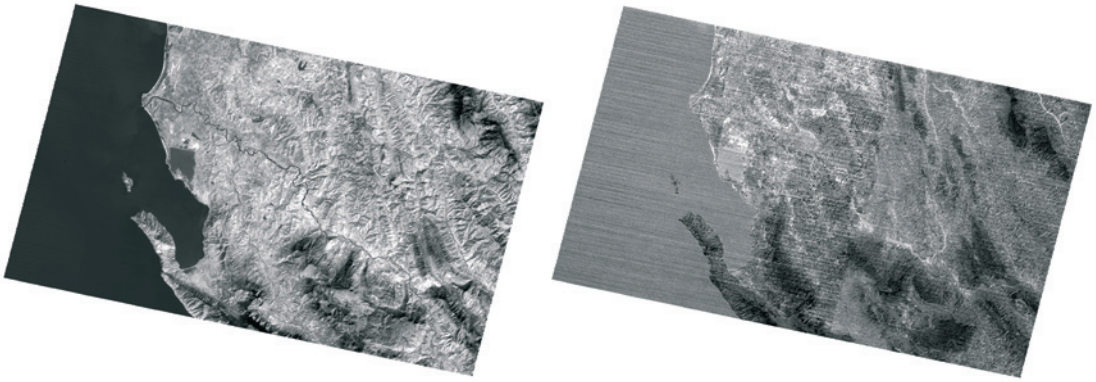

Figure 6 The first two principal component layers of the TIR ASTER bands displayed in gray tones (left image – PCA1, right image – PCA2)

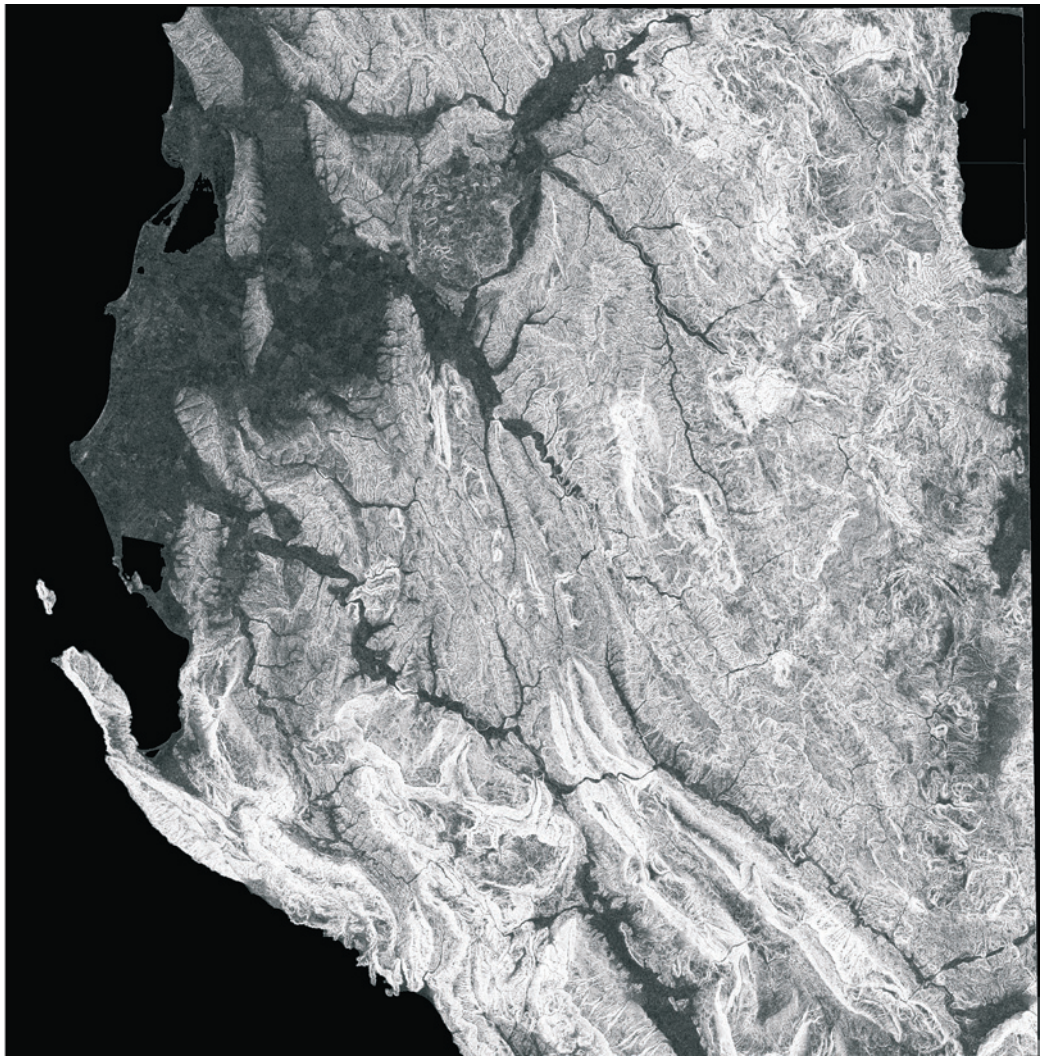

Figure 7 The slope derived layer of the DEM

in the upper left corner when overlaid (Fig. 5), can produce these visualization problems. This visual discontinuity of the pixel at the side areas of image happens:

- in the case of a different spatial resolution band composite image;
- in the case of a mosaic in a color composition of bands with different spatial resolution;
- when different spatial resolution bands are elaborated with the PCA algorithm.

Thermal infrared bands – TIR: as previously mentioned, the surface land temperatures may be of help in order to discover underground active structures. ASTER records this type of information with five specific bands (namely the TIR system). TIR system bands have a different spatial, spectral and radiometric resolution from all the other bands. In the TIR system case (as we did for VNIR and SWIR systems) we applied the PCA transformation to the ASTER mosaic in order to eliminate the interband correlation. The first two principal components explained 99.82% of the total variance. While PCA2 explains only 0.22% of variance, in this case we decided to consider only PCA1 for its predominant informative content. Figure 6 shows PCA1 and PCA2 of the TIR system. As can be observed, the right image (PCA2) is affected by noise and this, of course, restricts its informative content.

Digital Elevation Model – DEM – slope and aspect analysis: the slope layer (Fig. 7), enables one to verify the change in elevation over a certain distance (in this case 30 meters – the

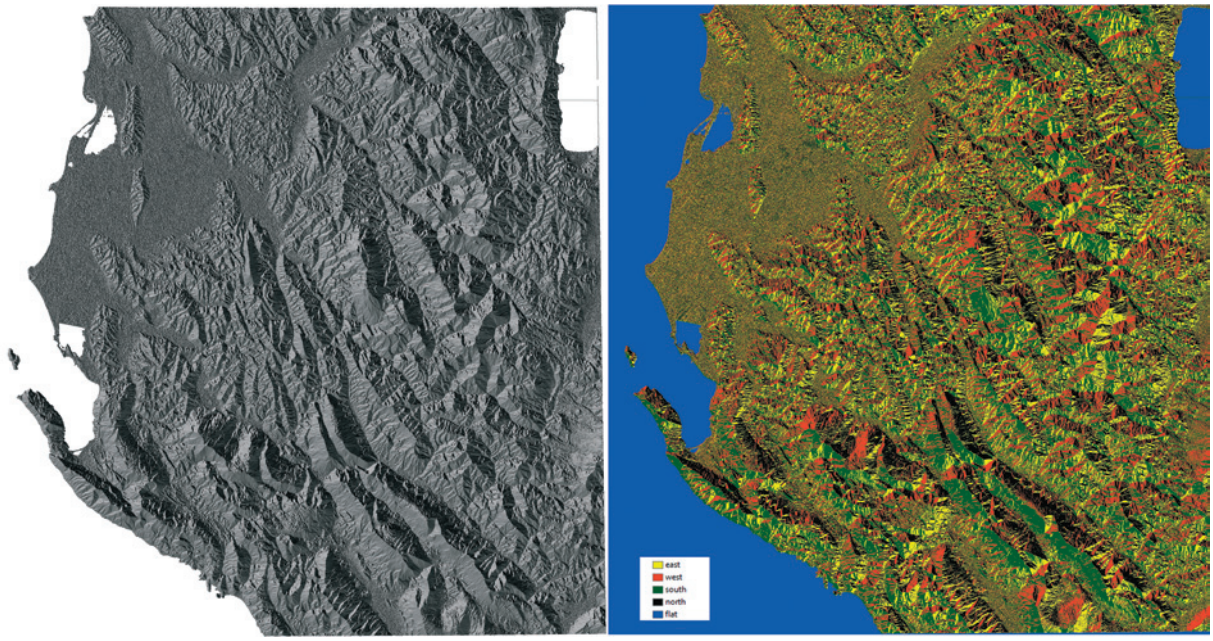

Figure 8 The aspect derived layer of the DEM (left image). The right image is the aspect layer classified in five classes: North, South, East West and Flat directions

spatial resolution of the DEM). It is expressed in percentage and is displayed in gray tones (dark: low slope, light: high slope). The aspect layer can be seen in Figure 8 (left image) and allows one to see the prevailing direction of the slope at each pixel. The image on the right (Fig. 8) shows the aspect layer classified in five classes of intervals: the four cardinal points and the flatlands. We did not introduce the half quarters in the classification (North/East, North/West, etc.) in order not to overcomplicate the map with an excessive number of symbols/tones. Furthermore, in Fig. 8 we can see the internal waters of the studied area in blue: the Ohrid Lake (top right of the image) and the Karavasta Lagoon (top left of the image, close to the coastline).

Raster layer analysis - Results

We carefully analyzed the produced raster layers in order to detect some possible surface anomalies, which can indicate the presence of an underground fault. This enabled us to identify several zones, in which the observation of sudden surface discontinuities, determined more or less marked alignments (mainly in the NW-SE direction). These alignments have been drawn on the basis of the different raster layers produced by the satellite scene analysis. The final result has been a vector layer with 30 suspected fault lines. Figure 9 shows the results of the analysis. The vector layer has been overlaid over the raster base layer. As base layer, we have chosen the PCA1 of the VNIR and SWIR system (already seen in frame 1 of Fig. 4), for visibility reasons.

In order to weigh the identified 30 fault lines in a way that underlines each fault line reliability, we scored each line. The score of each line is obtained by summing the raster layers on which the faults have been recognized inside. For instance: if a suspected fault line has been recognized on the basis of NDVI, PCA1 and DEM aspect layers, its score will be 3 (the sum of the three layers). Every suspected fault line can therefore be scored from 1 to 7, which was the total number of layers we investigated. These were as follows:

1. NDVI (Normalized Difference Vegetation Index);
2. PCA1 thermal (first principal component of TIR system);
3. PCA1 multispectral (first principal component of VNIR and SWIR systems);
4. PCA2 multispectral (second principal component of VNIR and SWIR systems);

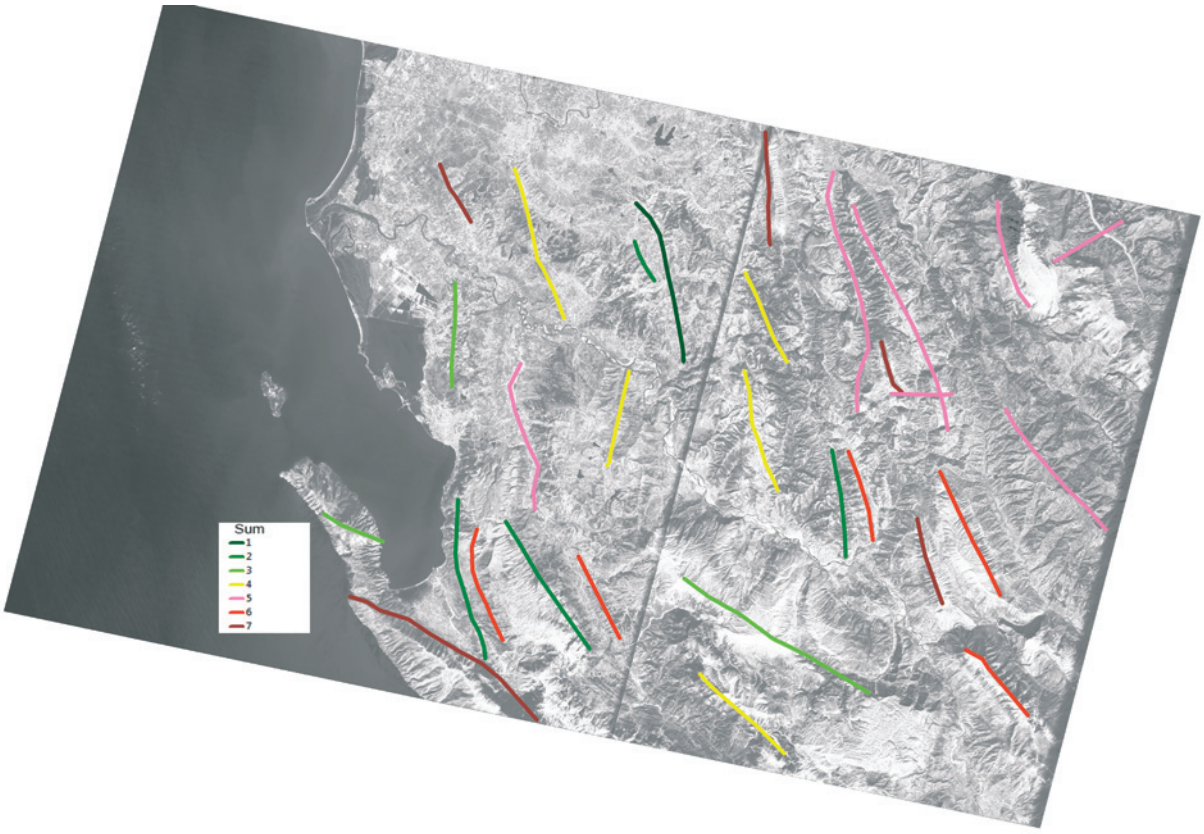

Figure 9 The base raster layer is PCA1 of the ASTER VNIR/SWIR bands displayed in gray tones. The overlaid vector layer is showing the suspected faults on the base of the satellite imagery elaboration. The linear faults have been weighted depending on the number of the layers on which the faults was recognized

5. PCA3 multispectral (third principal component of VNIR and SWIR systems);
6. DEM aspect (prevailing direction of the slope at each pixel);
7. DEM slope (change in elevation of each pixel);

We did not consider thermal PCA2 (system TIR) because of its poor informative content (see Fig. 6, right image). The different score fault lines have been graded by color on the map, from green (score 1 – less probable fault line) to brown (score 7 – more probable fault line).

First check of the results

We compared our results with the fault lines extracted from the Albanian Geological Survey, the bibliography maps and the geological sections interpreted from the seismic profiles. Fig. 10 shows the comparison. The base layer of the figure is again PCA1 (VNIR and SWIR systems). The vector layers in the legend are:

- "thrusts from the bibliography" in light blue – the layer of the thrusts extracted from the Albanian Geological Survey map (Xhomo et al., 1999; 2002) and the bibliography maps from Aliaj et al. (2000), Carcaillet et al. (2009), Velaj (2011);
- "geological sections" in black – the layer showing the location of two geological sections (interpreted from the seismic profiles and taken from Aliaj, 2006 and Arapi 2012);
- "fault points" in red – the point layer indicating the existence of an underground fault;
- "satellite rec. thrusts" in various colors – the layer indicating the 30 faults identified by the satellite imagery analysis, classified in 7 classes (low values – less probable fault; high values – more probable fault).

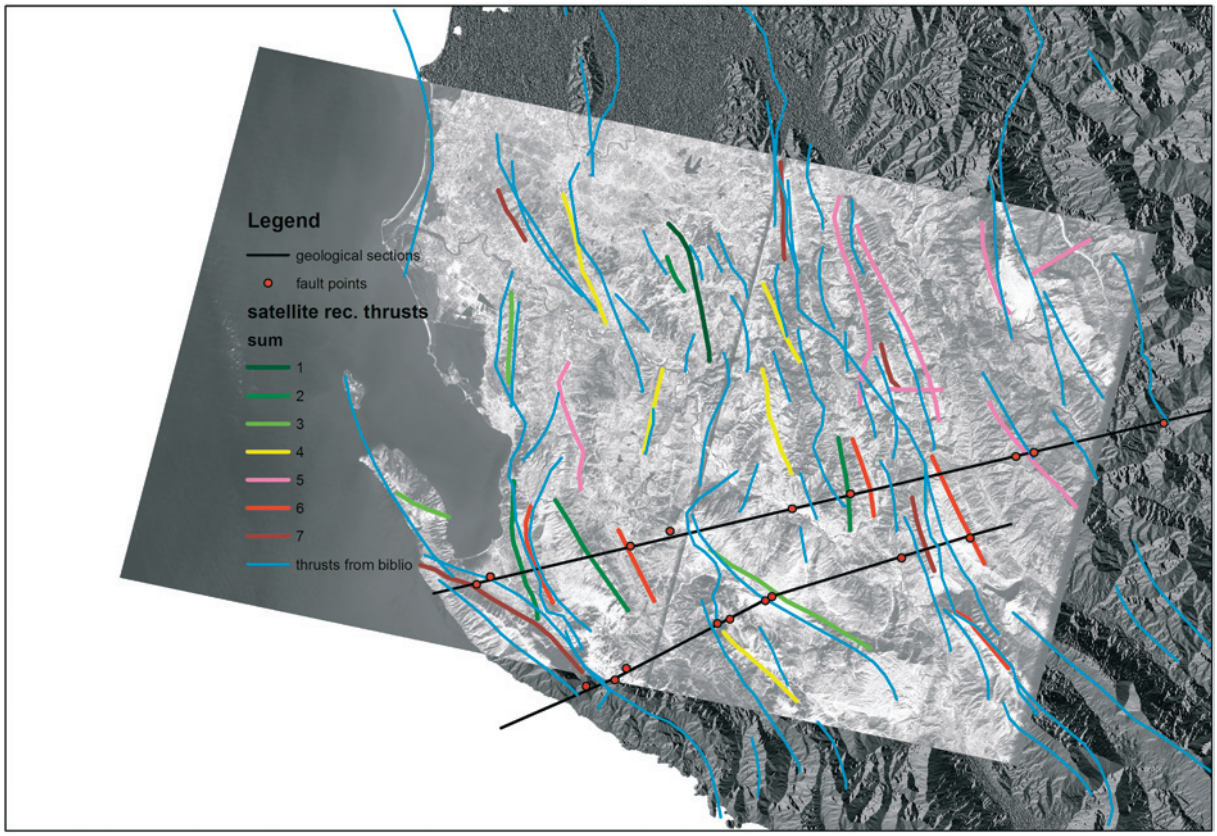

Figure 10 The base raster layer is PCA1 of the ASTER VNIR/SWIR bands displayed in gray tones. The overlaid vector layers are: the bibliography derived thrusts; the geological sections; the fault points on the geological sections (red balls); the 30 suspected faults classified on the basis on their visibility over each raster layer we elaborated from the ASTER data.

As it is evident in Figure 10, several fault lines have been identified. Some of them were already mapped in the bibliography, as for instance the great "y" shaped by two thrusts and one back thrust in the SW part of the image, near the Karaburun Peninsula. Also, the check of the identified thrusts along the geological sections seems to suggest a discrete congruity, especially if we check the location of the red points[4]. In the figure there are also several potential thrusts never mapped before, which will be eventually confirmed by future local surveys. In the particular case, this map could be of help as the starting point for a future local test by the National Institute of Oceanography and Experimental Geophysics researchers during the realization of a project in progress.

[4] The red points indicate surface faults that develop underground even 10 km in depth.

Conclusions

The aim of the paper was to show how a less invasive and relatively cheap technique, such as remote sensing, can be usefully used as a preliminary analysis in order to identify active faults in a certain area. The structural features of the faults together with the peculiarities of remote sensing methods render total automated analysis of the geologic phenomenon almost impossible. Geology qualified user participation is very important, almost more in this case with respect to the more traditional remote sensing uses, like for instance the land cover recognition or the verification of the vegetation health in a certain territory.

Nevertheless, it is possible to prepare in a semi-automated way some "semifinished product" (the raster layer we elaborated) which can be used in a following visual analysis. These raster layers can be very useful in order to detect an underground

fault on the basis of some surface evidences. An active fault can, for instance, bring to surface the underground waters, increasing in this way the vegetation. The same can connect soils with different lithologic features to the extent of leading to erosive morphologies and / or different steepness from zone to zone. The partial congruity of the obtained results, stemming from the starting point of the bibliographic data can be validated in the future by geologic analysis *in situ*, seems to suggest an optimism regarding the effectiveness of the adopted methodology.

Acknowledgements

The ASTER L1B data were obtained through the online Data Pool at the NASA Land Processes Distributed Active Archive Center (LP DAAC), USGS/Earth Resources Observation and Science (EROS) Center, Sioux Falls, South Dakota (https://lpdaac.usgs.gov/get_data).

BIBLIOGRAPHY

Aliaj, SH. (1998): *Neotectonic structure of Albania,* Albanian Journal of Natural & Technical Sciences, 4, 79-97.

Aliaj, SH. (2000): *Neotectonics and seismicity in Albania,* In Meco S., Aliaj S., Turku I. (eds): Geology of Albania, Gebruder Borntrager, Berlin, Beitrage zur regionalen Geologie der Erde, 2000, 28, 135-178.

Aliaj, SH. (2006): *The Albanian Orogen: convergence zone between Eurasia and the Adria Microplate,* In Pinter N., Grenerczy G., Weber J., Stein S. and Medak D. (eds): The Adria Microplate: GPS Geodesy, Tectonics and Hazards, NATO Sciences, Series IV: Earth and Environmental Sciences, Springer, Vol. 61, 133-149.

Aliaj, SH., Adams, J., Halchuk, S., Sulstarova, E., Peci, V., Muco, B. (2004): *Probabilistic seismic hazard maps for Albania,* 13th World Conference on Earthquake Engineering, Vancouver, B. C., Canada, August 1-6, 2004, Paper No. 2469.

Aliaj, SH., Sulstarova, E., Muço, B., Koçiu, S. (2000): *Seismotectonic Map of Albania*, scale 1:500.000, Seismological Institute, Tirana.

Arapi, A. (2012): *Petroleum Opportunities in ALBANIA,* Hydrocarbon Broshure edited by Albanian National Agency of Natural Resources (AKBN).

Campbell, J. B. (1996): *Introduction to Remote Sensing*, Taylor & Francis, London.

Carcaillet, J., Mugnier, J.L., Koçi, R., Jouanne, F. (2009): *Uplift and active tectonics of southern Albania inferred from incision of alluvial terraces,* Quaternary Research, doi:10.1016/j.yqres.2009.01.002.

Crósta, A. P., De Souza Filho, C. R., Azevedo, F., Brodie, C. (2003): T*argeting key alteration minerals in epithermal deposits in Patagonia, Argentina, using ASTER imagery and principal component analysis*, International Journal of Remote Sensing, 24/1, 4233-4240.

Frasheri, A., Bushati, S., Bare, V. (2009): *Geophysical outlook on structure of the Albanides,* Journal of the Balkan Geophysical Society, 12/1, 9-30.

Fu, B., Ninomiya, Y., Lei, X., Toda, S., Awata, Y. (2004): *Mapping active fault associated with the 2003 Mw 6.6 Bam (SE Iran) earthquake with ASTER 3D images*, Remote Sensing of Environment, 92, 2, 153-157.

Gomez, C., Delacourt, C., Allemand, P., Ledru, P., Wackerle, R. (2005): *Using ASTER remote sensing data set for geological mapping, in Namibia*, Physics and Chemistry of the Earth, Parts A/B/C, 30/1–3, 97-108.

Gupta, R. P. (2003): *Remote sensing Geology*, Springer, New York.

Hollenstein, C., Kahle, H. G., Geiger, A., Jenny, S., Goes, S., Giardini, D. (2003): *New GPS constraints on the Africa-Eurasia plate boundary zone in southern Italy,* Geophys. Res. lett., 30/18, 1935, doi: 10.1029/2003GL017554.

Jardin, A., Roure, F., Nikolla, L. (2011): *Subsalt depth seismic imaging and structural interpretation in Dumre area, Albania,* Oil & Gas Science and Technology, 66, 911-929.

Jensen, J. R. (2000): *Remote sensing of Environment*, Prentice Hall, New Jersey.

Jouanne, F., Mugnier, J. L., Koci, R., Bushati, S., Matev, K., Kuka, N., Shinko, I., Kociu, S., Duni, L., (2012): *GPS constraints on current tectonics of Albania,* Tectonophysics, 554-557, 50-62.

Lacombe, O., Malandain, J., Vilasi, N., Amrouch, K., Roure, F. (2009): *From paleostress to paleoburial in fold-thrust belts: Preliminary results from calcite twin analysis in the Outer Albanides,* Tectonophysics, 475, 128-141.

Lillesand, T. M., Kiefer, R. W. (1994): *Remote sensing and Image Interpretation*, Wiley &Sons, New York.

Mather, P. M. (1999): *Computer Processing of Remotely-Sensed Images*, Wiley, Chichester.

Moore, F., Rastmanesh, F., Asadi, H., Modabberi, S. (2008): *Mapping mineralogical alteration using principal component analysis and matched filter processing in the Takab area, north-west Iran, from ASTER data*, International Journal of Remote Sensing, 29/10, 2851-2867.

Nieuwland, D., Oudmayer, B. C., Valbona, U. (2001): *The tectonic development of Albania: explanation and prediction of structural style,* Marine and Petroleum Geology, 18, 161-177.

Papadaki, E. S., Mertikas, S. P., Sarris, A. (2011): *Identification of Lineaments with possible structural Origin using ASTER images and DEM derived Products in Western Crete*, Greece, EARSel eProceedings, 10, 1/2011.

Perez, F. G., Higgins, C. T., Real, C. R. (2006): *Evaluation Of Use Of Remote-Sensing Imagery In Refinement Of Geologic Mapping For Seismic Hazard Zoning In Northern Los Angeles County*, California, ISPRS Archives – Volume XXXVI Part 7.

Robertson, A., Shallo, M. (2000): *Mesozoic-Tertiary tectonic evolution of Albania in its region eastern Mediterranean context,* Tectonophysics, 316, 197-254.

Roure, F., Nazaj, S., Fili, I., Cadet, J. P., Mushka, K., Bonneau, M. (2004): *Kinematic evolution and Petroleum systems-an appraisal of the Outer Albanides*, AAPG Memoir 82, 474-493.

Rouse, J.W., Haas, R.H., Schell, J.A., Deering, D.W. (1974): *Monitoring vegetation systems in the Great Plains with ERTS*, Proceedings, Third Earth Resources Technology Satellite-1.

Sabins, F. (1996): *Remote Sensing*, *Principles and Interpretation*, Freeman, New York.

Sulstarova, E., Aliaj, SH. (2001): *Seismic hazard assessment in Albania,* Albania Journal of Natural & Technical Sciences, 10, 89-100.

Symposium, Greenbelt: NASA SP-351, 3010-3017.

Tarolli, P., Arrowsmith, J.R., Vivon, E.R. (2009): *Understanding Earth surface processes from remotely sensed digital terrain models*, Geomorphology, 113/1,2, 1-126.

Tarolli, P., Arrowsmith, J.R., Vivoni, E.R. (2009): *Understanding earth surface processes from remotely sensed digital terrain models*, Geomorphology, 113/1–3.

Van der Meer, F.D., Van der Werff, H.M.A., Van Ruitenbeek, F.J.A., Hecker, C.A., Bakker, W.H., Noomen, M.F., Van Der Meijde, M., Carranza, E.J.M., Boudewijn de Smeth, J., Woldai, T. (2012): *Multi- and hyperspectral geologic remote sensing: a review,* International Journal of Applied Earth Observation and Geoinformation, 14/ 1, 112-128.

Van Hinsbergen, D.J.J., Langereis, C.G., Meulenkamp, J.E. (2005): *Revision of the timing, Magnitude and distribution of Neogene rotations in the western Aegean region,* Tectonophysics, 396, 1-34.

Velaj, T. (2001): *Evaporites in Albania and their impact on the thrusting processes,* Journal of the Balkan Geophysical Society 4, 1, 9-18.

Velaj, T. (2011): *Tectonic Style in Western Albania Thrustbelt and Its Implication on Hydrocarbon Exploration,* AAPG International Convention and Exhibition, Milan, Italy, October 23-26, 2011.

Velaj, T., Davison, I., Serjani, A., Alsop, I. (1999): *Thrust tectonics and the role of evaporates in the Ionian Zone of the Albanides,* AAPG Bulletin 83/9, 1408-1425.

Vilasi, N., Malandain, J., Barrier, L., Callot, J.P., Amrouch, K., Guilhaumou, N., Lacombe, O., Muska, K., Roure, F., Swennen, R. (2009): *From outcrop and petrographic studies to basin-scale fluid flow modelling: The use of the Albanian natural laboratory for carbonate reservoir characterization,* Tectonophysics, 474, 367-392.

Wahi, M., Taj-Eddine, K., Laftouhi, N. (2013): *ASTER VNIR & SWIR Band Enhancement for Lithological Mapping - A case study of the Azegour Area (Western High Atlas, Morocco)*, Journal of Environment and Earth Science, 3/12, 33-44.

Walker, R.T. (2006): *A remote sensing study of active folding and faulting in southern Kerman province*, S.E. Iran, Journal of Structural Geology, 28, 654–668.

Xhomo, A., Kodra, A., Gjat, K., Xhafa Z., Dixon, E. (1999): *Tectonic Map of Albania*, scale 1:200.000, published by Council for Geoscience, RSA.

Xhomo, A., Kodra, A., Dimo, LL., Xhafa, Z., Nazaj, SH., Nakuçi, V., Yzeiraj, D., Lula, F., Sadushi, P., Shallo, M., Vranaj, A., Melo, V. (2002): *Harta gjeologjike e Shqiperise, Geological map of Albania*, scale 1:200,000, published by the Ministry of Industry and Energy, Republic of Albania.

Zelilidis, A., Piper, D.J.W., Vakala, I., Avramidis, P., Getsos, K. (2003): *Oil and gas plays in Albania: Do equivalent plays exist in Greece?*, Journal of Petroleum Geology, 26/1, 29-48.